Technical University of Denmark

Stiffened Plates and Sandwich Constructions
41517

Report B

Authors:
Christian Casarotto (s223302)
Irene Berganzo (s223230)

Instructor:
Prof. Christian Berggreen

May 8, 2023

Contents

Introduction **1**

1 Problem formulation **2**
1.1 Load definition 3

2 Method of analysis **4**
2.1 Assumptions 4
2.2 Governing equation 5
2.3 Fracture criteria 7

3 Material choice and models **9**
3.1 Load configurations 9
3.2 Material choice 9
3.3 Layout optimization 12

4 Results and discussions **14**
4.1 FEM model description 14
4.2 Analitical model validation with FEM 14
4.3 Finding critical plate 16
4.4 Optimization 17

List of Figures **I**

List of Tables **I**

References **I**

5 Appendix **II**

Introduction

The following document describes the preliminary study and design of a transport helicopter floor. The study starts with the definition of the problem, where the engineering assumption are described and the problem is outlined. Following this the analysis method are briefly introduced and the Matlab code is validate using a FEM model for both orthotropic and isotopic sandwich plates.
Material choice is done exploring several configurations, from composite to aluminium sandwich construction, following the criteria of weight minimization, long life and reduced cost. Other aspects like wear and fire are also considered towards the end of the document, following a comparison with more classical solutions, as single skin composite and metal skins.

Danmarks Tekniske Universitet DTU

1 Problem formulation

The studied helicopter floor is connected with a stiffened sub-structure, represented in appendix A. The sub-structure carries all the global loads, like for instance forces in the take-off and landing phase, therefore the floor only needs to sustain the payload associated forces.
The floor is composed of three main panels, referred to as panel (a), (b) and (c) in figure 1, connected to the sub-structure. As no further specification is given these are assumed to be bolted to the substructure, in order to be removable for substitution or maintenance purposes. To conduct the analysis each main panel is divided in sub-panels, supported by the underneath webs. These are named as is figure 1.
The three main panels are considered as independently fixed to the bulkheads, which are treated as infinitely stiff, therefore all the external edges can be considered as clamped. The intermediate webs corresponding to internal lines offer support to the main panels. If these are rigidly fixed on the intermediate webs, they could be considered as clamped there, but if the panels are able to rotate around the webs, they are better approximated by simply supported boundary condition.

Nevertheless, as the aim of this study is to only perform a preliminary analysis, focusing on the sandwich structure and material to be used, all the edges are considered as simply supported in this document. More detailed analysis are saved for further steps of the design process, focusing this first analysis on a conservative approach of all simply supported boundary conditions.

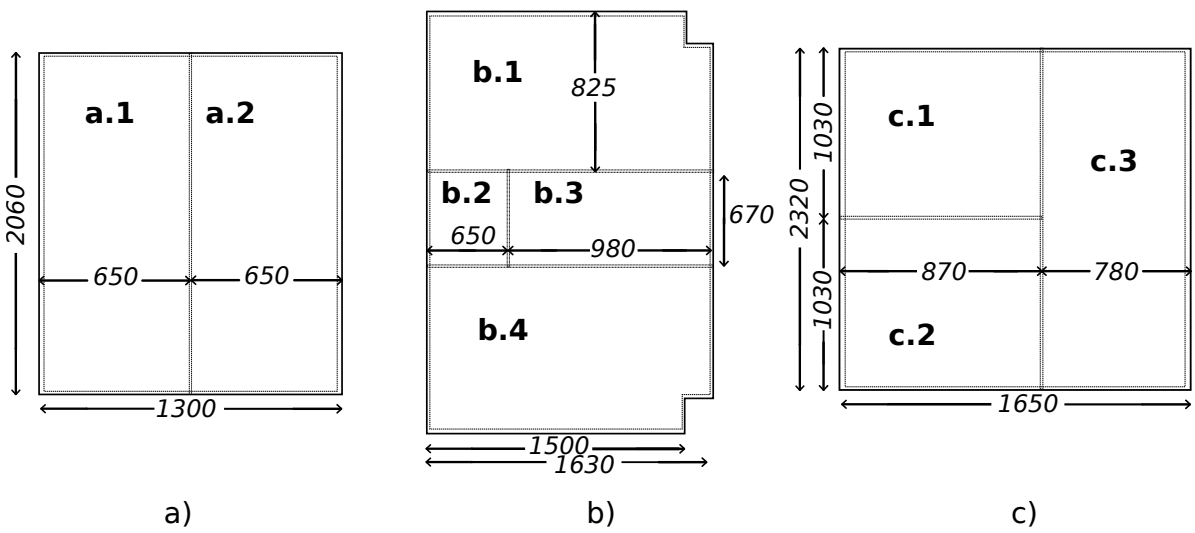

Figure 1: Dimensions of the helicopter floor

Following the technical specifications the measures in figure 1 are given. These are conservative approximations of the real dimensions, reported in appendix B, where for instance the web width of the sub-structure is not considered. Each sub-panel in figure 1 is considered as an independent simply supported panel and analyzed individually in section 3.
Plates *b.1* and *b.4* present a pointy 90° corner on the supports, which might cause stress

concentration in the sandwich plates. As this can be critical for the panels in a load carrying helicopter it is safe to assume that the corner will be reinforced and/or some supports will be integrated to distribute the load in that area of the panels. In this preliminary study panels *b.1* and *b.4* are considered neglecting the corner, so as 1500x825 mm panels.

1.1 Load definition

The floor must be able to withstand the following loads:

- An 800 kg/m^2 evenly distributed load over the entire floor
- A downwards acceleration of 4.5g
- Fuel tank pressure of 3.00 kPa, acting upwards on the floor when the tanks are full
- A local load of 100 N acting on an area of 100 mm^2

As the fuel tank pressure is directed upwards in the panel reference system this helps reducing the deflection, and will therefore be neglected in first instance. Any eventual compression on the floor given by the fuel is neglected, as in this scenario deflection loads are more relevant. Also it is safe to assume that in a helicopter the fuel tank is well enclosed in a robust space, and therefore the fuel pressure is not directly applied underneath the floor.
Local loads are particularly critical for sandwich panels, and to be conservative they will be considered in the center of the plate. The floor thickness should not exceed 30mm, and a safety factor 1.5 is used against material failure. For metallic sheet materials, the allowable load case is considered as the yielding point, but for composite materials an additional factor of 1.2 is used due to the fragile behaviour and lack of yielding. The floor should also be stiff enough to give safety feeling when walking on it, with deflection not over 25 mm.
The design criteria for the helicopter floor are in order of importance low weight, long life and low cost. Also, aspects like manufacturing methods, wear and fire resistance are considered.

Danmarks Tekniske Universitet DTU

2 Method of analysis

For the sake of brevity no general introduction on sandwich structures is given in this chapter, where the focus is on the approximations and methods used for the analysis.
Sandwich structures are used in weight critical components, without renouncing to high resistance and toughness. They rely on what in the literature is often referred to as *sandwich effect*, which consists in optimizing the material distribution moving it towards the extremes. This is done in plates as well, to reach the highest possible flexural rigidity D with a given material. This becomes evident when looking at equation 2.1, which describes the flexural rigidity of a plate. Here the Steiner's theorem component, D_0, dominates on the others.
Here E is the young modulus and d the distance between face sheets.

$$D = \sum_{i=1}^{3} E_i l_i = \frac{E_f t_f^3}{6} + \frac{E_f t_f d^2}{2} + \frac{E_c t_c^3}{12} = 2D_f + D_0 + D_c \tag{2.1}$$

2.1 Assumptions

In sandwich structures the best performance to weight combination is found in the "weak core and thin face sheets configuration". This maximizes D_0 minimizing the utilized material, and also allows for further simplification of the used formulas. The condition is met for the threshold of thinness and weakness described in equations 2.2.

$$3\left(\frac{d}{t_f}\right)^2 > 100 \text{ or } \frac{d}{t_f} > 5.77 \qquad \frac{6 \cdot E_f \cdot t_f \cdot d^2}{E_c \cdot t_c^3} > 100 \tag{2.2}$$

Following these criteria D_f and D_c are negligible due to the values of t_f and E_c in faces and core, which will be low to save weight. This condition also results in approximations in the stress distribution. In the case of a weak core, it assumes that all the normal stresses and bending moments are absorbed by the face sheets, while thin face sheets assume that all the shear loads and transverse forces are absorbed by the core.
Throughout all the study the "weak core and thin face sheets configuration" condition is met, even if not specified, as the presented methods are in part simplified using this assumption.

In classic uniform plates and structures shear deformation is generally negligible in a bending scenario, accounting for less that 5% of the total deformation w. As this is not the case for sandwich plates, where deformation due to shear and due to bending are close ($w_s \simeq w_b$), one needs to account not only for bending stiffness D, but also shear stiffness S. In first approximation and following the thin face sheets and weak core assumption, w_s and w_b can be considered to occur exclusively in core and face sheets respectively.

The explored material solutions for the helicopter floor include orthotropic configurations, like honeycomb cores and fiber reinforced face sheets. Here the formulas for the orthotropic case are presented, as are used for all the analyzed cases.
A list of material parameters are introduced to fully characterize a sandwich plate.

Danmarks Tekniske Universitet DTU

- Flexural rigidities in all the directions, D_x, D_y and D_{xy}. Equations 2.3 and 2.4.
- Shear stiffness in x and y direction, S_x and S_y, which are assumed to be constant along the cross section. Equations 2.5.
- Poisson ratios for the plate in xy an yx directions, respectively ν_{xy} and ν_{yx}. These can be taken as $\nu = \nu_{xy} = \nu_{yx}$ for isotropic face sheets, or with the approximation in equations 2.6 otherwise.

Following the made assumptions of thin face sheets and weak core, these parameters can be found with the listed equations 2.3 to 2.6. Following these considerations the materials can be defined with the parameters listed below.

$$D_x \simeq \frac{E_{x1} \cdot t_1 \cdot E_{x2} \cdot t_2 \cdot d^2}{E_{x1} \cdot t_1 + E_{x2} \cdot t_2} \qquad D_y \simeq \frac{E_{y1} \cdot t_1 \cdot E_{y2} \cdot t_2 \cdot d^2}{E_{y1} \cdot t_1 + E_{y2} \cdot t_2} \tag{2.3}$$

$$D_{xy} \simeq \frac{2 \cdot G_{xy1} \cdot t_1 \cdot G_{xy2} \cdot t_2 \cdot d^2}{G_{xy1} \cdot t_1 + G_{xy2} \cdot t_2} \tag{2.4}$$

$$S_x \simeq \frac{G_{cx} \cdot d^2}{t_c} \qquad S_y \simeq \frac{G_{cy} \cdot d^2}{t_c} \tag{2.5}$$

$$\nu_{xy} \simeq 0.25 \cdot \sqrt{\frac{D_x}{D_y}} \qquad \nu_{yx} = \nu_{xy} \cdot \frac{D_x}{D_y} \tag{2.6}$$

- Face sheets: young modulus of the two faces in all the directions: E_{x1}, E_{y1}, E_{x2}, E_{y2}; and shear modulus G_{xy1} and G_{xy2}.
- Core: Shear modulus in x and y: G_{cx}, G_{cy}; and young modulus E_{cx}, E_{cy} and E_c, mostly used to check weak core condition and when testing compressive failure criteria.

Other assumptions are that d is constant, so there is no compression of the core that would lead to change in face sheet distance. Also the material properties are considered constant along the plate.

2.2 Governing equation

In this analysis the tool for sandwich plate deflection problems is the First Order Shear Deformation Theory (FSDT). This comes with the assumption discussed in section 2.1, to simplify the otherwise lengthy equations.

To find the governing equation, one has to superimpose the deflection effects due to shear and bending, $w = w_b + w_s$, and compute the equilibrium of forces in the plate. An overview of the forces is given in figure 2.

Danmarks Tekniske Universitet DTU

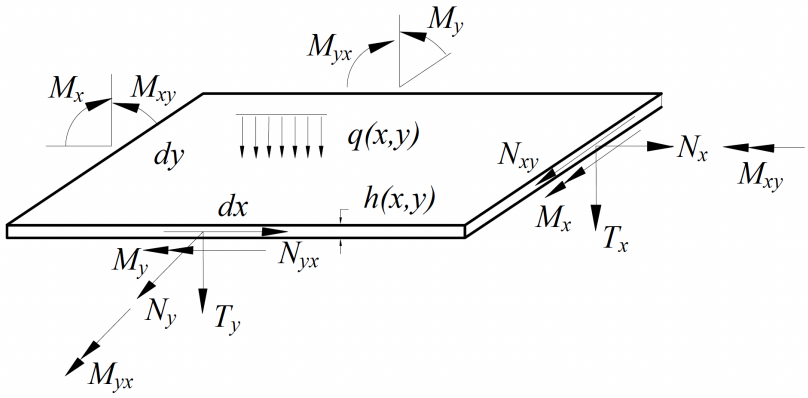

Figure 2: Loads and forces in a plate [1]

In orthotropic plates transfer forces, moments and deflections are found assuming an expansion. Despite the method being only a first order approximation the equations are quite long, and parameters W_{mn}, X_{mn}, Y_{mn} and Z_{mn} are reported in appendix appendix C. The equations for deflection, transverse forces and moments are listed below.

$$T_x = \sum_{n=1}^{\infty}\sum_{m=1}^{\infty} \frac{X_{mn} q_{mn}}{Z_{mn}} \cos\left(\frac{m\pi x}{a}\right) \sin\left(\frac{n\pi y}{b}\right) \tag{2.7}$$

$$T_y = \sum_{n=1}^{\infty}\sum_{m=1}^{\infty} -\frac{Y_{mn} q_{mn}}{Z_{mn}} \sin\left(\frac{m\pi x}{a}\right) \cos\left(\frac{n\pi y}{b}\right) \tag{2.8}$$

$$w = \sum_{n=1}^{\infty}\sum_{m=1}^{\infty} -\frac{W_{mn} q_{mn}}{Z_{mn}} \sin\left(\frac{m\pi x}{a}\right) \sin\left(\frac{n\pi y}{b}\right) \tag{2.9}$$

$$\begin{aligned} M_x = \sum_{n=1}^{\infty}\sum_{m=1}^{\infty} \frac{-D_x}{1-\nu_{xy}\nu_{yx}} \Bigg[W_{mn} \left\{ \left(\frac{m\pi}{a}\right)^2 + \nu_{yx} \left(\frac{n\pi}{b}\right)^2 \right\} + \left(\frac{m\pi}{a}\right) \frac{X_{mn}}{S_x} \\ - \nu_{yx} \left(\frac{n\pi}{b}\right) \frac{Y_{mn}}{S_y} \Bigg] \frac{q_{mn}}{Z_{mn}} \sin\frac{m\pi x}{a} \sin\frac{n\pi y}{b} \end{aligned} \tag{2.10}$$

$$\begin{aligned} M_y = \sum_{n=1}^{\infty}\sum_{m=1}^{\infty} \frac{-D_y}{1-\nu_{xy}\nu_{yx}} \Bigg[W_{mn} \left\{ \left(\frac{n\pi}{b}\right)^2 + \nu_{xy} \left(\frac{m\pi}{a}\right)^2 \right\} - \left(\frac{n\pi}{b}\right) \frac{Y_{mn}}{S_y} \\ + \nu_{xy} \left(\frac{m\pi}{a}\right) \frac{X_{mn}}{S_x} \Bigg] \frac{q_{mn}}{Z_{mn}} \sin\frac{m\pi x}{a} \sin\frac{n\pi y}{b} \end{aligned} \tag{2.11}$$

Danmarks Tekniske Universitet DTU

$$M_{xy} = -\frac{D_{xy}}{2}\left(\frac{\partial}{\partial x}\left(\frac{\partial w}{\partial y} - \frac{T_y}{S_y}\right) + \frac{\partial}{\partial y}\left(\frac{\partial w}{\partial x} - \frac{T_x}{S_x}\right)\right) \tag{2.12}$$

As usually q_{mn} is the one in equation 2.13, where q is the distributed load on the plate. As the loads in the helicopter floor are both distributed and static, these will be considered by adding $q_{mn,dist}$ and $q_{mn,con}$, changing the integration extremes of the latter. These are the equations that will be used throughout all the analysis in this document, and they refer to the simply supported boundary condition, as anticipated in section 1. In sandwich plates it is also necessary to distinguish between soft and hard boundary conditions, where in the first one shear strain is allowed along the edges and in the second it is blocked. In the case of a floor the shear strain is blocked and the plate can instead experience torsional moment, leading to hard boundary conditions.

$$q_{mn} = \frac{4}{ab}\int_0^a \int_0^b q \sin\left(\frac{m\pi x}{a}\right) \sin\left(\frac{n\pi y}{b}\right) dy\, dx \tag{2.13}$$

The resulting stresses, following the assumption of chapter 2.1, are in equations 2.14 to 2.16. Here only the tensile stress for one face sheet is reported as the other one is similar.
As stated in chapter 1 the overall forces on the helicopter are absorbed by the substructure, so the normal forces N_x and N_y are null in these equations, leading to very simple equations for the stresses on the floor.

$$\sigma_{fx1} \approx \frac{N_x E_{x1}}{E_{x1}t_1 + E_{xc}t_c + E_{x2}t_2} - \frac{M_x}{t_1 d} \tag{2.14}$$

$$\sigma_{fy1} \approx \frac{N_y E_{y1}}{E_{y1}t_1 + E_{yc}t_c + E_{y2}t_2} - \frac{M_y}{t_1 d} \tag{2.15}$$

$$\tau_{fxy} \approx \pm\frac{M_{xy}}{t_f d} \qquad \tau_{cyz} = \frac{T_y}{d} \qquad \tau_{cxz} = \frac{T_x}{d} \tag{2.16}$$

2.3 Fracture criteria

There are several fracture criteria to consider depending on the type of load and type of sandwich structure. Face and core fracture and local indentation are among the most critical cases for the floor panels, as they sustain both distributed and concentrated loads. Phenomena like global buckling or shear crimping can be neglected as there is no overall normal loads on the plates. Nevertheless, one still needs to consider wrinkling and face dimpling, as localized buckling can happen due to deflection associated stresses on the face sheets.

The criteria for face fracture differ depending on the type of material. For metallic materials one can take advantage of isotropy and use Mohr's circles to find the maximum

Danmarks Tekniske Universitet DTU

principal stress, equation 2.17. This is then compared with the critical stress for the metal, accounting for a safety factor.
For core fracture, thanks to the assumptions, one only needs to verify that the shear stresses do not exceed the material limit. This is done in equation 2.18 considering of course the transverse forces (similar for T_x and T_y). When using orthotropic composite face sheets, equation 2.17 is not sufficient to check for face fracture. In this scenario, classical lamination theory must be used, coupled with a different criteria like the Hoffman fracture criteria. The description of these methods is neglected in this document.

$$\sigma_{\mathrm{cr}} = \frac{\sigma_{\mathrm{fx}} + \sigma_{\mathrm{fy}}}{2} + \sqrt{\left(\frac{\sigma_{\mathrm{fx}} - \sigma_{\mathrm{fy}}}{2}\right)^2 + \tau_{\mathrm{fxy}}^2} \qquad (2.17) \qquad\qquad \tau_{cr,xz} = \frac{T_x}{d} \qquad (2.18)$$

Local indentation is a risk mainly due to the presence of the localized 100N load. The approach for foam cores is very simple, as one can find the resulting compressive stress and compare it with the critical one of the core, therefore considering no contribution from the face sheets.

Wrinkling is a critical type of localized buckling, which might occur in the upper face sheets of the floor panels due to compression. As this leads to failure of the face sheet, it is important to use conservative formulas as equations 2.19 to find the critical loads, it being in the x or y direction. These are valid for all types of face sheets and materials.

$$\sigma_{\mathrm{crx}} = 0.5 \cdot \sqrt[3]{E_{\mathrm{x}} \cdot E_{\mathrm{cx}} \cdot G_{\mathrm{cx}}} \qquad \text{or} \qquad \sigma_{\mathrm{cry}} = 0.5 \cdot \sqrt[3]{E_{\mathrm{y}} \cdot E_{\mathrm{cy}} \cdot G_{\mathrm{cy}}} \qquad (2.19)$$

Face dimpling is also a localized type of buckling, but it does not bring to failure of the structure. It it characteristic of honeycomb cores, as it occurs in between the cells and depends by their dimension. The formula used to find the critical load for hexagonal cells is 2.20.

$$\sigma_{\mathrm{cr}} = \frac{2E_f}{1 - \nu_f^2} \cdot \left(\frac{t_f}{s}\right)^2 \qquad (2.20)$$

Danmarks Tekniske Universitet DTU

3 Material choice and models

Critical criteria have been provided to select the material for the structure. In order of importance, low weight is the most crucial property to consider, followed by long life and price. The manufacturing method and different damaging phenomena like wear and fire must also be considered.

3.1 Load configurations

The floor will be subjected to a weight of $800kg/m^2$ which will be $7.85kPa$. It will also suffer a downwards acceleration of $4.5g$, which taking the weight into account leads to a pressure of $35.3kPa$. A fuel tank pressure of $3kPa$ acting upwards when the tanks are full. Finally, a local load of $100N$ acting on an area of $100mm^2$, which results in a localized pressure of $1MPa$. Therefore, different situations will happen where the loads will interact with each other. They can be divided into two main situations: still and downwards accelerated during a hard landing. For both of them, 4 different sub-situations can be found in function of the loads acting: weight only; weight and fuel tank (which will be in opposites directions so it will be less critical); weight and local pressure; and finally the weight, fuel and local pressure all at the same time, as described in table 1.

In sandwich structures local loads are especially dangerous for core indentation and local fracture of the sandwich. Nevertheless, with the most critical scenario being the hard landing, the local $1MPa$ load has be added to the distributed $35.3MPa$ pressure resulting from the payload. Also, to enhance the conservative approach, the local load is preventively placed in the middle of the plates during the calculations, as this is the most critical condition.

Loads	Criticality condition
Weight (↓)	4
Weight(↓) + fuel(↑)	3
Weight(↓) + local(↓)	1
Weight(↓) + fuel(↑) + local(↓)	2

Table 1: Load conditions

As evident from table 1 the most critical condition is the one of hard landing without considering fuel pressure. That will be $35.3kPa$ distributed load and local $1MPa$ load acting in the middle of the plate.

3.2 Material choice

Having defined the loads it is now time to conduct a materials study for the floor panels. Some of the most commonly used materials for face sheets are aluminium alloys, carbon fibres, glass fibres and many others. For core applications the main distinction can be done between foams and honeycomb structures in aeronautical applications, with the first being the most affordable and practical ones and the latter the most high performing.

As stated previously the most important parameter for the floor is low weight. In the frameworks of material choice this translates into low density, which is the parameter used for comparison.

To evaluate long life in the floor panes, the chosen parameter is Young modulus E. This is certainly not a definitive parameter to evaluate the long-term resistance of a component, but it can be a good approximation for a preliminary study. One could consider fracture toughness as a better long life estimator, but this is a more complex parameter to asses, and will therefore be left as a suggestion for the next steps of the floor design, not considered in this document.

Cost is the last of the main criteria. Approximations for costs of the material can be easily found in the literature, and will be used directly in the material selection process.

To have a uniform source of data as reference, the Ansys Granta EduPack software is used as data source for the material parameters, in order of importance density, Young modulus and cost. These are retrieved for a selection of materials, divided into face sheets and core materials, grouped in tables 2 and 3.

FACE OPTIONS	Density [kg/m^3]	E_x [GPa]	Price [EUR/kg]
Carbon fiber UD	1490	1.21E+02	37.4 - 41.6
Carbon fiber woven	1420	61.34	37.4 - 41.6
Epoxy E-Glass UD	2000	45	24.3 - 34.4
Magnesium AZ31B	1770 - 1780	44 - 46	7.74 - 8.73
Aluminium 2024 T2	2.75e3 - 2.78e3	72 - 75.7	3.23 - 4.32
Titanium Ti-6Al-4V	4420 - 4430	111 - 119	21.7 - 27
304 Stainless steel	7610 - 7870	190 - 210	4.15 - 4.59

Table 2: Face sheets options with data

For the face sheets, in between metals, aluminum and magnesium offer great performance and relatively low density. In between the two magnesium seems to be the favourite, as cost in only the last of the choice criteria, and E is still high despite the low density. Despite this magnesium is probably not the best choice for this application, because of wear and especially fire hazard which is something that does not happen with aluminum. As the main criteria is low density, from table 2 it is evident that fiber reinforced composites (FRC) offer a much lower weight than aluminium, with similar mechanical properties. In between carbon fiber and glass fiber, the choice falls in carbon fiber, due to higher performance and lower weight. Carbon fiber also offers the possibility to optimize the ply layout, as described in section 3.3.

For the core material selection, E modulus is substituted by shear modulus G. This is due to the fact the the core of a sandwich structure is mostly loaded in shear and therefore E is not determinant as a material parameter. A good example of this are honeycomb structures: the E modulus of a honeycomb core will always be very small compared for example to a foam, but the G modulus is much higher, offering great shear toughness.

Danmarks Tekniske Universitet DTU

CORE OPTIONS	Density [kg/m^3]	G_{xy} [GPa]	Price [EUR/kg]
Aluminium honeycomb 0.025	25.1 - 26.1	0.138 - 0.152	16.8 - 28
Aluminium honeycomb 0.05	48 - 54.4	0.296 - 0.345	16.8 - 28
Aluminium honeycomb 0.097	94.9 - 98.7	0.635 - 0.702	16.8 - 28
Nomex Honeycomb 0.024	23 - 24	0.016 - 0.021	29.7 - 41.9
Nomex Honeycomb 0.05	48 - 50	0.03 - 0.058	29.7 - 41.9
Nomex Honeycomb 0.096	94.1 - 97.9	0.0676 - 0.0931	29.7 - 41.9
Polystyrene (EPS) 0.03	28 - 32	0.0035 - 0.005	2.78 - 3.06
PVC Foam	36 - 44	0.01 - 0.016	15.3 - 16.9
Polyurethane Foam 0.062	59.2 - 64	0.00366 - 0.00503	9.97 - 11
PET Foam	235 - 245	0.0475 - 0.0525	10.2 - 11.3
Aluminum Foam	970 - 1.08e3	5 - 5.5	8.29 - 10.4

Table 3: Core options with data

For core materials, PVC and EPS foams are interesting in terms of density, but offers too low strength for the floor panels. At a much higher cost the Nomex honeycomb offers very low density compared to the foams, but for a similar density the most logical choice from table 3 is to use aluminum honeycomb 0.025, which also comes at a lower cost.

The final choice for the sandwich panels to be employed in the helicopter floor is to use carbon fiber face sheets and aluminum honeycomb core 0.025.

The carbon fiber face sheets are optimized in section 3.3, while for the core the final mechanical properties are already made available in table 4. All the parameters are given from the Ansys Granta database, computing an average of the given range.

E_z [GPa]	E_x [GPa]	E_y [GPa]	G_{xy} [GPa]	G_{yx} [GPa]	ν_{xy} [/]	ν_{yx} [/]
0.138	3.81e-5	9.12e-5	0.145	0.0758	0.465	0.465

Table 4: Mechanical properties of aluminum honeycomb 0.025

In terms of maximum allowable stresses, this type of honeycomb offers a compressive strength of 0.673 MPa, shear strength of 0.586 MPa in the xz direction and 0.345 MPa in the yz direction.

From these values it is already evident that a problem arises. The compressive strength is way lower that the compression given by the the point load, which as discussed in section 3.1 is equivalent to 1MPa. Especially if we consider the 1.5 safety factor, this means that the aluminum honeycomb 0.025 core is definitely not sufficiently strong for the load, thus needs to be changed.

Coming back to table 3, other possible light choices are Nomex honeycomb 0.024, for which the compressive strength is 0.66 MPa, so still not sufficient, or PVC foam, which offers a 0.4 MPa compressive strength. The most natural choice falls then again in the second aluminum honeycomb, the 0.05 with a density of roughly 51 kg/m^3. This is going to

Danmarks Tekniske Universitet DTU

be the core of the sandwich panels. The properties are presented in table 5, again taking an average. For this honeycomb core the compressive strength is 2.31 MPa, so safely far from the 1 MPa threshold, also if considering the safety factor. The shear strength in xz direction is 1.5 MPa and in the yz direction is 0.946 MPa.

E_z [GPa]	E_x [GPa]	E_y [GPa]	G_{xy} [GPa]	G_{yx} [GPa]	ν_{xy} [/]	ν_{yx} [/]
0.552	3.05e-4	7.395e-4	0.3205	0.155	0.465	0.465

Table 5: Mechanical properties of aluminum honeycomb 0.05

3.3 Layout optimization

Having chosen the material for the face sheets, i.e. epoxy/HS carbon fiber UD prepreg, one can proceed to find the optimal layup of the sheets to minimize the deflection, and therefore stresses. Layout optimization can be dealt with using classic lamination theory, which exceeds the intention of this document, therefore only a few considerations are made in this section. The material parameters for the unidirectional ply are reported in table 6

E_x [GPa]	E_y [GPa]	G_{xy} [GPa]	ν_{xy} [/]
121	0.86	4.7e-3	0.27

Table 6: Unidirectional ply properties

One of the great advantages of using fiber composites is that the engineer can tune the fiber layout to reach the optimal performance. With the simply aim to get the best layout in terms of deflection and stresses, a simple distributed load of 1kPa is considered in this section, acting on a simply supported sandwich panels with the core in table 5.

Observing the nine plates in figure 1, it is evident that they divide in between roughly squared plates and elongated ones. It is then interesting to test the ply layout effect on the two cases, and find the more optimal solution. This is done using a Matlab code where classical lamination theory is implemented, allowing for faster calculations in this sense.

Taken a 500x500 mm plate for the squared one and 1500x500 mm as example of the elongated plate, one can fix the single ply thickness to 0.2 mm and using four plies and 10 mm thick core test each layout. This is done in tables 7 and 8. The used layouts and results are listed in the tables, yielding to the interesting conclusion that a [0 45 -45 90] ply layout is beneficial for squared plates, but represents the worst configuration for elongated ones instead. This seems logical, as the most similarly-isotropic configuration is the one best fitting the plate with uniform shape. Also, the [0 90 90 0] is the best configuration for the elongated plates, which fits the idea of stiffening the longest direction to avoid large deflections there. Also it is interesting to observe how shear stress increases in the face sheet when its deflection decreases.

Danmarks Tekniske Universitet DTU

Layup	Deflection [mm]	σ_{fx} [MPa]	σ_{fy} [MPa]	τ_f [MPa]
[0 90 90 0]	0.2875	1.559	2.843	5.202e-04
[0 30 60 90]	0.2034	1.738	1.402	0.743
[0 45 -45 90]	0.1927	1.564	1.285	0.899

Table 7: Layout optimization - squared plate

Layup	Deflection [mm]	σ_{fx} [MPa]	σ_{fy} [MPa]	τ_f [MPa]
[0 90 90 0]	0.3782	0.0364	3.754	5.225e-04
[0 30 60 90]	0.5163	1.024	3.562	1.079
[0 45 -45 90]	0.5234	1.326	3.420	1.380

Table 8: Layout optimization - elongated plate

The conclusions from this brief layout optimization are that for further and elaborated optimization one could use a [0 90 90 0] layout for elongated plates and a [0 45 -45 90] in simil-square plates.

In the rest of the analysis, the [0 45 -45 90] layout is chosen as the definitive ply layout for the face sheets. This is to simplify the analysis and also to avoid excessive complexity in the floor manufacturing and assembly.

With this being chosen the final material parameters for the face sheets are calculated with the Matlab code (CLT) and reported in table 9, using four plies of same thickness in the discussed configuration. These will be implemented in the code for the final optimization, together with the stress limits to be used in the Hoffman fracture criterion, which are again taken from Ansys workbench engineering data, for unidirectional epoxy carbon fibre.

E_x [GPa]	E_y [GPa]	G_{xy} [GPa]	ν_{xy} [/]
4.0593e+04	4.0593e+04	1.5185e+04	0.3366

Table 9: Face sheets properties - [0 45 -45 90]

Danmarks Tekniske Universitet DTU

4 Results and discussions

Having chosen the materials for the sandwich structure, the next step of the analysis is to optimize it with respect to the applied loads, with the aim to reach the lowest weight. This involves implementing the theories presented in chapter 2 in a Matlab code, able to iterate the calculations for different core and face sheets thickness.

In section 4.1, a short description of the FEM model is presented, and in section 4.2, this FEM model is used to validate the analytical model developed in Matlab, to assess the quality of the implementation. After this, in section 4.3, all the nine plates illustrated in figure 1 are implemented to find the most critical point of the floor structure, which will be used as reference. Found the critical points, the structure is optimized in section 4.4.

4.1 FEM model description

The software used for the numerical model is ANSYS, with the ACP tool specifically developed to design and analyse layered composites. The model has been created following some input data described next.

Dimensions used for the plate are 500x500 mm; a mesh for the shell plate with elements of 5mm squares, leading to 10201 number of nodes and 10000 number of elements. To add the specific "hard boundary" condition on ANSYS, it has been set a 0 mm displacement for all the nodes on the edges on Z direction; the upper and down edges' nodes have 0 rotation in the Y direction and the right and left edges' nodes have a 0 rotation along X direction; the node of the middle has the in-plane displacement fixed, only being allowed to move translate along Z axis, and a node in the middle of the edge has been restricted in the direction of the edge.

Apart from the boundary conditions and dimensions of the mesh, a uniformly distributed load of 10 kN has been added on one of the faces. The sandwich materials for the validation are described later, as it depends on the specific model which is being validated. The numerical model is almost ready to run.

4.2 Analitical model validation with FEM

As mentioned before, to asses the Matlab implementation, three sample plate problems are implemented in numerical and analytical models, to compare the results. The following results for tables 10 and 10 are calculated by the two methods in the middle point of one of the face sheets for the σ_1 and σ_2, therefore the principal stresses in the 2 directions, and in the corners for τ in order to obtain the maximum values.

The isotropic case consists in a sandwich plate with aluminum face sheets, E 71000 MPa, G 26692 MPa and ν=0.33, and for the core, PVC foam E 70 MPa, G 26.92 MPa and ν=0.3.

For the orthotropic cases, two options have been modelled. Model 1 with the same aluminium face sheet mentioned before (isotropic), and a honeycomb provided by the program, being $E_1 = 1$ MPa, $E_2 = 1$ MPa, $E_3 = 255$ MPa; $G_{12} = 1$ MPa, $G_{23} = 37$ MPa, $G_{13} = 70$ MPa and $\nu_{12} = 0.49$, $\nu_{23} = 0.01$ and $\nu_{13} = 0.01$ the data which will be used for the analytical

calculation as well. In this last case, the weak core condition was not being fulfilled, therefore core thickness has been decreased to 18 mm. The orthotropic Model 2 has been developed with carbon fibre composite in the faces stacked in the structure [0, 45, -45, 90], keeping the original thickness on the face of 1 mm and 20 mm on the core.

	ISOTROPIC			ORTHOTROPIC model 1		
	Analytical	Numerical	Error %	Analytical	Numerical	Error %
w [mm]	0.4548	0.40403	12.5	0.3610	0.3606	0.4
σ_x [MPa]	-5.8324	-5.9368	1.8	-7.3074	-7.6823	4.9
σ_y [MPa]	-5.8324	-5.9368	1.8	-5.5852	-5.2854	5.7
τ_c [MPa]	0.0794	0.0776	11.1	0.0923	0.0919	0.4

Table 10: Comparision between numerical and analytical models

	ORTHOTROPIC model 2		
	Analytical	Numerical	Error %
w [mm]	0.2667	0.2523	5.7
σ_x [MPa]	-3.2378	-3.4612	6.4
σ_y [MPa]	-2.3571	-0.5947	390
τ_c [MPa]	0.081	0.081	0

Table 11: Comparision between numerical and analytical models

Next, some pictures of the orthotropic numerical model 1 can be found.

Danmarks Tekniske Universitet DTU

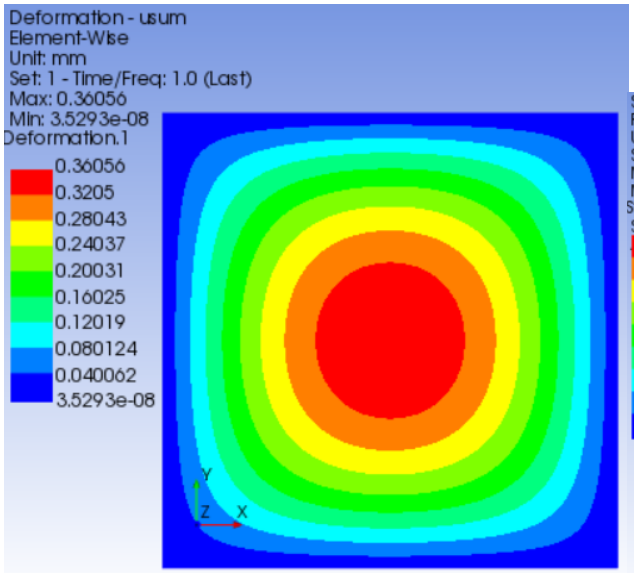

Figure 3: Plot of deflection in the model 1 orthotropic.

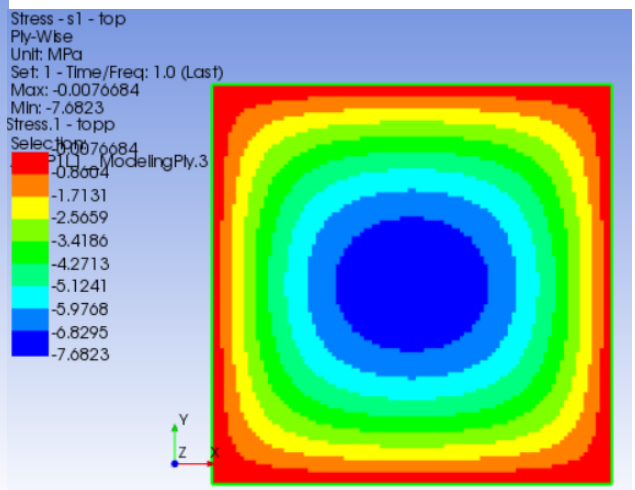

Figure 4: Plot of σ_x in the second face sheet bottom

The discrepancies are low for isotropic conditions, being the analytical model more conservative than the numerical in deflection and shear stress, but slightly less conservative for the stresses in the principal directions (less than 2 % of difference). The numerical model supports the conclusions of the analytical model.

Regarding the orthotropic models, both methods bring similar solution values for deflection and stresses, with around 5 % error. Note that there is an unusual error for the σ_2 in the model 2; it may be due to a wrong interpretation of the numerical method solution.

The analytical model developed in Matlab is considered validated for the next steps of the design.

4.3 Finding critical plate

Using the maximum load configuration presented in table 1, it is now possible to test where in the nine plates from figure 1 the critical points are. Unfortunately this is not limited to verifying the maximum deflection point w_{max} in each plate. Instead, following the fracture criteria described in section 2.3, it is evident that maximum tension σ_{max} and shear τ_{max} are needed, to check for both face and core fracture and local buckling phenomena. As σ_{max}, τ_{max} and w_{max} might be in different plates and in different locations within the plate, all the nine of them have been implemented in the Matlab code, with the aim to find the coordinates of the desired points. In these points the optimization will run, to reduce the thickness of the plate, therefore reducing its weight.

The plates were tested in the order presented in the initial schematic, figure 1, and with the reported dimensions. The applied loads are the ones described in section 3.1,

Danmarks Tekniske Universitet DTU

corresponding to an uniformly distributed pressure of 35.3 kPa and a point load on 100N in an area of 100 mm^2, which is considered in the center of the plate as a conservative approach.

The material is the definitive design choice, corresponding to aluminium honeycomb 0.05 core, whose properties are described in table 5, and carbon fiber face sheets, with properties in table 9 and [0 45 -45 90] layout as previously discussed.

As initial choice for the face sheets, a thickness of 4 mm was chosen, with proportional ply thickness, each of which will be 1 mm thick. The core is initially chosen to be 22 mm thick, yielding the overall thickness of the sandwich to 30 mm, corresponding to the design constrain. From these valued the dimensions will then be lowered approaching the critical limit.

The coordinates are reported in table 12, where the maximum tensile and shear stresses from the two directions are simply referred to as σ and τ. The coordinates will be used as reference in the rest of the study. An example of 3D plot to identify the parameters is given in figure 5 and 6 for maximum tension and shear stress respectively.

	Deflection w		Tension σ		Shear τ	
coordinate	x [mm]	y [mm]	x [mm]	y [mm]	x [mm]	y [mm]
b.1 - b.4	815	412.5				
c.3			515	435	515	0

Table 12: Coordinates of maximum stresses

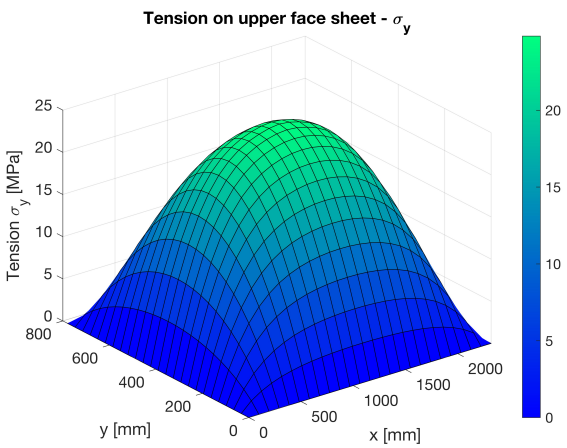

Figure 5: Plot of σ_y in the face sheets - c.3

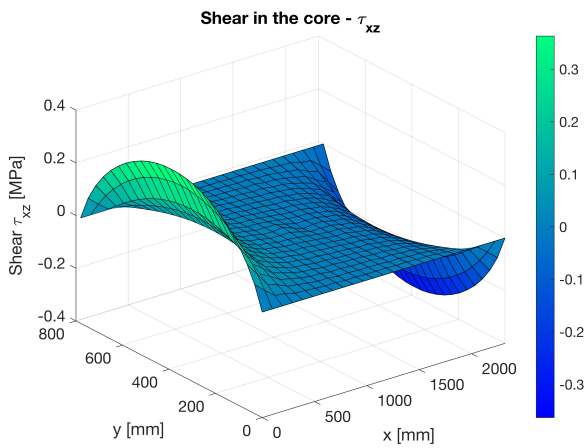

Figure 6: Plot of τ_x in the core - c.3

4.4 Optimization

At this point the next step in the design process is to optimize the weight of the floor, reducing thickness of the core and of the face sheets. This involves getting closer to the

Danmarks Tekniske Universitet DTU

material limits, and checking for all the different fracture criteria described in section 2.3.

Deflection, tensile stress and shear stress are checked in two different plates and in the coordinates listed in table 12. These were found to be the critical spots of the entire floor in the most critical load condition.

At this point in the process a problem was encountered. Face fracture for carbon fiber material makes use of the classic lamination theory (CLT), and an external Matlab code was implemented to use Hoffman's fracture criteria for the face sheets. Due to time constrain it was not possible to correctly adapt this external code to check for face fracture. As in this situation it would only be possible to check for the other failure criteria, it was preferable to change material, using a metallic face sheets, for which the analytical implementation was ready and secured.

The face sheet material is then changed to normal isotropic aluminum, with $E = 71000$ MPa in both x and y direction and $G = 26692$ MPa as shear modulus. The Poisson ratio for this type of material is $\nu = 0.33$. The core is kept the same, so the aluminum honeycomb 0.05 whose characteristics are described in table 5. The ratio of the circle inside the honeycomb cell is taken as 5mm, a good equilibrium between price and performance. With this material, $sigma_y = 270$ MPa as yielding stress and 1.5 as safety factor, it was possible to run a dimension optimization.

The first optimization was for the deflection in plates b.1 and b.4, which as stated in section 1.1 shouldn't exceed 25 mm. Running some iterations it is found that the plate reaches fracture well before reaching that level of deflection, so no further analysis is needed.

For plate c.3 the test is run for shear and tensile stress. To avoid core fracture due to the shear stress the thickness needs to be roughly 12 mm. For the face sheets, the most critical phenomena is found to be wrinkling. To avoid this, the best thickness is found as roughly 2 mm.

Using this combination of 12 mm core and 2 mm face sheets, the structure should not collapse. One could run a more optimized choice of thickness for core and face sheets, bringing every plate to the material limit. This type of analysis is not described here, as considered for future evolution of this preliminary study. Also, for the sake of design simplicity, it might be not worth to change thickness of the components for each sandwich panel, as this would further increase the complexity.

Danmarks Tekniske Universitet DTU

List of Figures

1 Dimensions of the helicopter floor 2
2 Loads and forces in a plate [1] 6
3 Plot of deflection in the model 1 orthotropic. 16
4 Plot of σ_x in the second face sheet bottom 16
5 Plot of σ_y in the face sheets - c.3 17
6 Plot of τ_x in the core - c.3 17
7 Schematic view of the substructure II
8 Schematic view of the three main panels and sub-panels with measures . . . III
9 Schematic view of the three main panels with measures III

List of Tables

1 Load conditions 9
2 Face sheets options with data 10
3 Core options with data 11
4 Mechanical properties of aluminum honeycomb 0.025 11
5 Mechanical properties of aluminum honeycomb 0.05 12
6 Unidirectional ply properties 12
7 Layout optimization - squared plate 13
8 Layout optimization - elongated plate 13
9 Face sheets properties - [0 45 -45 90] 13
10 Comparision between numerical and analytical models 15
11 Comparision between numerical and analytical models 15
12 Coordinates of maximum stresses 17

References

[1] D. Zenkert, *The Handbook of Sandwich Construction.* KTH, School of Engineering Sciences (SCI), 1997.

Danmarks Tekniske Universitet DTU

5 Appendix

Appendix A - Helicopter substructure representation

The following drawing is a schematic view of the helicopter sub-structure. Here the areas where the three main panels and their sub-panels are fixed is visible, and the intermediate webs are highlighted. This part of the helicopter is meant not only to support the floor but also to carry all the general loads that occur during operation, and that will therefore not be felt by the floor panels.

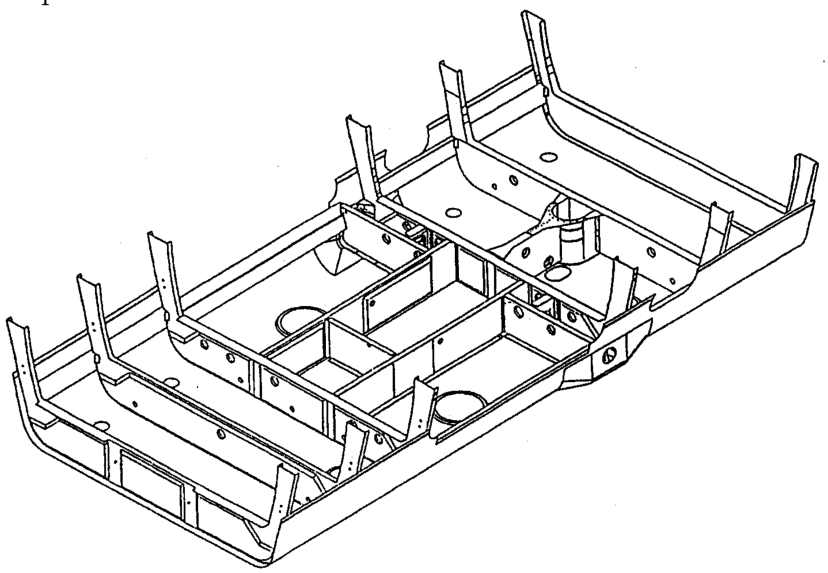

Figure 7: Schematic view of the substructure

Appendix B - Panel specification

The following figures report a schematic view of the three main floor panels and their sub-panels, with the given measures. All the measures are in millimeters and the quotes are given in between center-lines of the webs. Each web has a width of 50 mm. The non shaded areas are inspection hatches and the black dotted lines are joins between sub-panels.

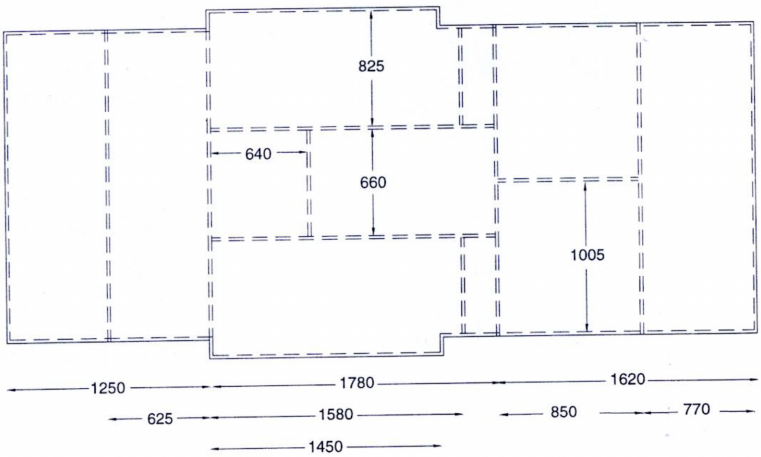

Figure 8: Schematic view of the three main panels and sub-panels with measures

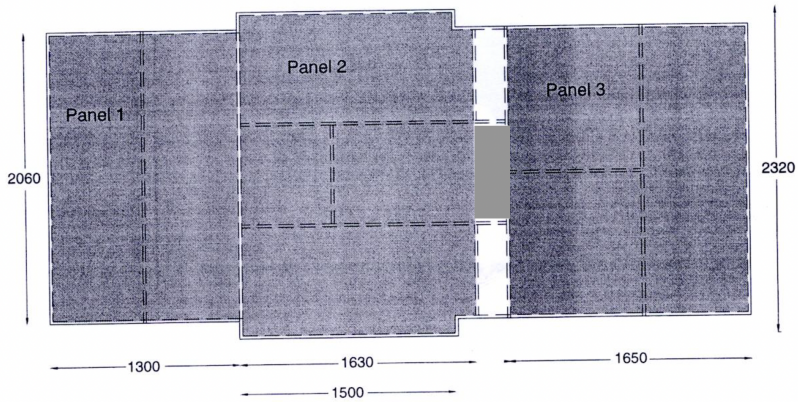

Figure 9: Schematic view of the three main panels with measures

Appendix C - constants for the orthotropic solution

What follows is the equations for the W_{mn}, X_{mn}, Y_{mn} and Z_{mn} coefficients. These are used in the load calculations for the orthotropic simply supported sandwich plate, as described in this document.

$$W_{mn} = -\frac{1}{S_x S_y}\left[\frac{1}{2}D_{xy}\left\{\begin{array}{l}\left(\frac{m\pi}{a}\right)^4 \frac{D_x}{1-v_{xy}v_{yx}} - \left(\frac{m\pi}{a}\right)^2\left(\frac{n\pi}{b}\right)^2 \frac{v_{xy}D_x+v_{yx}D_y}{1-v_{xy}v_{yx}} + \\ \left(\frac{n\pi}{b}\right)^4 \frac{D_y}{1-v_{xy}v_{yx}}\end{array}\right\}\right.$$
$$\left. + \left(\frac{m\pi}{a}\right)^2\left(\frac{n\pi}{b}\right)^2 \frac{D_x D_y}{1-v_{xy}v_{yx}}\right] - \left[\left(\frac{m\pi}{a}\right)^2 \frac{D_x}{S_x\left(1-v_{xy}v_{yx}\right)} + \left(\frac{n\pi}{b}\right)^2 \frac{D_y}{S_y\left(1-v_{xy}v_{yx}\right)}\right]$$
$$-\frac{1}{2}D_{xy}\left[\frac{1}{S_y}\left(\frac{m\pi}{a}\right)^2 + \frac{1}{S_x}\left(\frac{n\pi}{b}\right)^2\right] - 1$$

$$X_{mn} = \frac{1}{S_y}\left(\frac{1}{2}\left(\frac{m\pi}{a}\right)^5 \frac{D_x \cdot D_{xy}}{1 - v_{xy}v_{yx}} + \left(\frac{m\pi}{a}\right)^3 \left(\frac{n\pi}{b}\right)^2 \left(\frac{D_x \cdot D_y}{1 - v_{xy}v_{yx}} - \frac{D_{xy} \cdot (v_{xy}D_x + v_{yx}D_y)}{2(1 - v_{xy}v_{yx})}\right) + \frac{1}{2}\left(\frac{m\pi}{a}\right)\left(\frac{n\pi}{b}\right)^4 \frac{D_y \cdot D_{xy}}{1 - v_{xy}v_{yx}} + S_y\left(\frac{m\pi}{a}\right)\left(\left(\frac{m\pi}{a}\right)^2 \frac{D_x}{1 - v_{xy}v_{yx}} + \left(\frac{n\pi}{b}\right)^2 \left(D_{xy} + \frac{v_{yx}D_x}{1 - v_{xy}v_{yx}}\right)\right)\right)$$

$$Y_{mn} = \frac{1}{S_x}\left(-\frac{1}{2}\left(\frac{n\pi}{b}\right)^5 \frac{D_y \cdot D_{xy}}{1 - v_{xy}v_{yx}} - \left(\frac{m\pi}{a}\right)^2 \left(\frac{n\pi}{b}\right)^3 \left(\frac{D_x \cdot D_y}{1 - v_{xy}v_{yx}} - \frac{D_{xy} \cdot (v_{xy}D_x + v_{yx}D_y)}{2(1 - v_{xy}v_{yx})}\right) - \frac{1}{2}\left(\frac{m\pi}{a}\right)^4 \left(\frac{n\pi}{b}\right) \frac{D_x \cdot D_{xy}}{1 - v_{xy}v_{yx}} - S_x\left(\frac{n\pi}{b}\right)\left(\left(\frac{n\pi}{b}\right)^2 \frac{D_y}{1 - v_{xy}v_{yx}} + \left(\frac{m\pi}{a}\right)^2 \left(D_{xy} + \frac{v_{xy}D_y}{1 - v_{xy}v_{yx}}\right)\right)\right)$$

$$Z_{mn} = \left(\frac{m\pi}{a}\right) X_{mn} - \left(\frac{n\pi}{b}\right) Y_{mn}$$